*Inorg. Chem.* **2004**, *43*, 2503–2514


# A Structural and Electrochemical Investigation of 1-Alkyl-3-methylimidazolium Salts of the Nitratodioxouranate(VI) Anions $[\{UO_2(NO_3)_2\}_2(\mu_4\text{-}C_2O_4)]^{2-}$, $[UO_2(NO_3)_3]^-$, and $[UO_2(NO_3)_4]^{2-}$

**Antonia E. Bradley,[†] Christopher Hardacre,*[,†] Mark Nieuwenhuyzen,[†] William R. Pitner,[†] David Sanders,[†] Kenneth R. Seddon,[†] and Robert C. Thied[‡]**

*The QUILL Centre, The School of Chemistry, Queen's University Belfast, Stranmillis Road, Belfast BT9 5AG, Northern Ireland, United Kingdom, and British Nuclear Fuels plc, B170 Sellafield, Seascale, Cumbria CA20 1PG, United Kingdom*

Received November 21, 2003

The properties of the 1-butyl-3-methylimidazolium salt of the dinuclear $\mu_4$-(*O*,*O*,*O*′,*O*′-ethane-1,2-dioato)bis[bis(nitrato-*O*,*O*)dioxouranate(VI)] anion have been investigated using electrochemistry, single-crystal X-ray crystallography, and extended X-ray absorbance fine structure spectroscopy: the anion structures from these last two techniques are in excellent agreement with each other. Electrochemical reduction of the complex leads to the a two-electron metal-centered reduction of U(VI) to U(IV), and the production of $UO_2$, or a complex containing $UO_2$. Under normal conditions, this leads to the coating of the electrode with a passivating film. The presence of volatile organic compounds in the ionic liquids 1-alkyl-3-methylimidazolium nitrate (where the 1-alkyl chain was methyl, ethyl, propyl, butyl, pentyl, hexyl, dodecyl, hexadecyl, or octadecyl) during the oxidative dissolution of uranium(IV) oxide led to the formation of a yellow precipitate. To understand the effect of the cation upon the composition and structure of the precipitates, 1-alkyl-3-methylimidazolium salts of a number of nitratodioxouranate(VI) complexes were synthesized and then analyzed using X-ray crystallography. It was demonstrated that the length of the 1-alkyl chain played an important *role*, not only in the composition of the complex salt, but also in the synthesis of dinuclear anions containing the bridging $\mu_4$-(*O*,*O*,*O*′,*O*′-ethane-1,2-dioato), or oxalato, ligand, by protecting it from further oxidation.

## Introduction

Volatile organic compounds (VOCs) have been linked to several air pollution problems including smog, ozone depletion, and groundwater contamination.[1] VOCs are commonly used by industry as solvents in chemical processes. In the nuclear industry, for example, organic diluents are used in reprocessing irradiated nuclear fuel.[2] The relatively low boiling points of VOCs aid their removal after the process, but hamper quantitative recovery of the solvent and make storage difficult. Due to their low vapor pressures, organic salts with relatively low melting points, often referred to in the literature as ionic liquids,[3] are currently being investigated as replacements for VOCs in an increasing number of chemical processes. The large number of reviews covering the field of ionic liquids[4] is evidence of the increasing academic and industrial interest in the subject of ionic liquids.

An accelerating number of papers demonstrate the growing interest in the use of first- and second-generation ionic liquids by the nuclear industry.[5−11] For example, the electrochemical

* Author to whom correspondence should be addressed. Phone: +44 28 9027 4592. Fax: +44 28 9038 2117. E-mail: c.hardacre@qub.ac.uk (C.H.); k.seddon@qub.ac.uk (K.R.S.).
† Queen's University Belfast.
‡ British Nuclear Fuels plc.

(1) Cann, M. C.; Connelly, M. W. *Real-world Cases in Green Chemistry*; American Chemical Society: Washington, DC, 2000.

(2) Dennis, I. S.; Jeapes, A. P. In *The Nuclear Fuel Cycle: From Ore to Waste*; Wilson, P. D., Ed.; Oxford University Press: Oxford, 1996; p 124.

(3) In this paper, the term "ionic liquid" refers solely to salts of organic cations with melting points below 100 °C. Such materials have been given a variety of names in the literature, e.g., liquid organic salts, ambient (or room) temperature molten salts, and nonaqueous ionic liquids. The 1-alkyl-3-methylimidazolium ionic liquids under investigation in this paper will be referred to as $[C_n\text{mim}]X$, where *n* is the number of carbons in the linear 1-alkyl group and X is either chloride or nitrate.

(4) (a) Welton, T. *Chem. Rev.* **1999**, *99*, 2071−2083. (b) Holbrey, J. D.; Seddon, K. R. *Clean Prod. Processes* **1999**, *1*, 223−236. (c) Rooney, D. W.; Seddon, K. R. In *Handbook of Solvents*; Wypych, G., Ed.; ChemTec Publishing: Toronto, Ontario, Canada, 2000; p 1459. (d) Wasserscheid, P.; Keim, W. *Angew. Chem., Int. Ed.* **2000**, *39*, 3772−3789. (e) Earle, M. J.; Seddon, K. R. *Pure Appl. Chem.* **2000**, *70*, 1391−1398. (f) *Ionic Liquids in Synthesis*; Wasserscheid, P., Welton, T., Eds.; Wiley-VCH: Weinheim, Germany.

10.1021/ic035350b CCC: $27.50 
Published on Web 03/18/2004

and spectrochemical behaviors of dioxouranium(VI) and dioxoplutonate(VI) species have been studied in chloroaluminate ionic liquids for the potential use of ionic liquids throughout the nuclear industry.[5,6] Recently, second-generation ionic liquids, which are hydrolytically much more stable, have been shown to efficiently extract metal species from aqueous media.[7] This is an area of great significance to the nuclear industry, which currently uses solvent extraction in the PUREX process for reprocessing spent nuclear fuel.[8] The chemistry of lanthanides in first- and second-generation ionic liquids, including the electrodeposition of these metals, has been the subject of a number of papers.[9] Critical mass calculations performed by Harmon et al. on mixtures of plutonium metal in chloroaluminate- and $[BF_4]^-$-based ionic liquids have also recently been published.[10] Recent work from our laboratories has led to the publication of a series of patents[11] and papers[12] concerned with using ionic liquids in nuclear fuel reprocessing and molten salt waste treatment.

The nuclear industry's interest in the oxalate anion, $[C_2O_4]^{2-}$, centers around its use as a thermally labile ligand and/or a precipitating agent.[13] In a recent paper,[12a] we reported the preparation of the novel dinuclear dioxouranium(VI) salt containing a bridging oxalate ligand, 1-butyl-3-methylimidazolium $\mu_4$-(*O*,*O*,*O*′,*O*′-ethane-1,2-dioato)-bis{bis(nitrato-*O*′,*O*)dioxouranate(VI)} ($[C_4mim]_2[\{UO_2(NO_3)_2\}_2(\mu\text{-}C_2O_4)]$), by the oxidative dissolution of uranium(IV) oxide in $[C_4mim][NO_3]$ using concentrated nitric acid as the oxidizing agent. The paper only reported the structure of the solid, as determined by X-ray crystallography, with no information on the speciation of the complex in solution.

In this paper, we describe an attempt to isolate the uranium from the $[C_4mim][NO_3]$ medium through electrochemical reduction to an oxouranium(IV) species. To examine the effects of changes to the length of the 1-alkyl group of the cation on the composition and structure of the dioxouranium(VI) complexes formed, the structures of a series of 1-alkyl-3-methylimidazolium dioxouranium(VI) salts (alkyl = $C_nH_{2n+1}$; $n = 1-6$, 12, or 16) were also determined. In addition, we describe an EXAFS investigation of the species formed in solution following oxidative dissolution of $UO_2$ in $[C_4mim][NO_3]$.

## Experimental Section

**Sample Preparation.** The 1-alkyl-3-methylimidazolium chlorides $[C_nmim]Cl$ ($n = 1-8$, 10, 12, 16, or 18) were prepared through the reaction of the appropriate chloroalkane with 1-methylimidazole, as has been previously described.[14] The 1-alkyl-3-methylimidazolium nitrates $[C_nmim][NO_3]$ ($n = 1-8$, 10, 12, 16, or 18) were prepared by metathesis reactions between silver(I) nitrate and the appropriate $[C_nmim]Cl$, carried out in water. The silver(I) chloride precipitate was removed by filtration from the aqueous mixture, and the water was removed from the $[C_nmim][NO_3]$ by evaporation under reduced pressure. To remove as much residual silver chloride as possible, the $[C_nmim][NO_3]$ was repeatedly dissolved in ethanenitrile and mixed with decolorizing charcoal, which acts as an effective nucleation site for the precipitation of silver chloride. The charcoal was removed by filtration, and the ethanenitrile was removed by evaporation under reduced pressure.

The preparation of $[C_4mim]_2[\{UO_2(NO_3)_2\}_2(\mu\text{-}C_2O_4)]$ has previously been described in detail.[12a] This method was adapted to produce complexes containing dioxouranium(VI) and the $[C_nmim]^+$ cations. In general, the procedure involved mixing $[C_nmim][NO_3]$ (10 g), uranium(IV) nitrate hexahydrate (1 g), concentrated nitric


(5) (a) Dewaele, R.; Heerman, L.; D'Olieslager, W. *J. Electroanal. Chem.* **1982**, *142*, 137−146. (b) Heerman, L.; Dewaele, R.; D'Olieslager, W. *J. Electroanal. Chem.* **1985**, *193*, 289−294.

(6) (a) Hitchcock, P. B.; Mohammed, T. J.; Seddon, K. R.; Zora, J. A.; Hussey, C. L.; Ward, E. H. *Inorg. Chim. Acta* **1986**, *113*, L25−L26. (b) Dai, S.; Toth, L. M.; Hayes, G. R.; Peterson, J. R. *Inorg. Chim. Acta* **1997**, *256*, 143−145. (c) Dai, S.; Shin, Y. S.; Toth, L. M.; Barnes, C. E. *Inorg. Chem.* **1997**, *36*, 4900−4902. (d) Anderson, C. J.; Choppin, G. R.; Pruett, D. J.; Costa, D.; Smith, W. *Radiochim. Acta* **1999**, *84*, 31−36. (e) Costa, D. A.; Smith, W. H.; Dewey, H. J. In *Molten Salts XII: Proceedings of the International Symposium*; Trulove, P. C., De Long, H. C., Stafford, G. R., Deki, S., Eds.; The Electrochemical Society: Pennington, NJ, 2000; p 80. (f) Hopkins, T. A.; Berg, J. M.; Costa, D. A.; Smith, W. H.; Dewey, H. J. *Inorg. Chem.* **2001**, *40*, 1820−1825. (g) Oldham, W. J.; Costa, D. A.; Smith, W. H. In *Ionic Liquids as Green Solvents: Progress and Prospects*; Rogers, R. D., Seddon, K. R., Eds; ACS Symposium Series 818; American Chemical Society: Washington, DC, 2002; pp 188−198.

(7) (a) Dai, S.; Ju, Y. H.; Barnes, C. E. *J. Chem. Soc., Dalton Trans.* **1999**, 1201−1202. (b) Visser, A. E.; Swatloski, R. P.; Reichert, W. M.; Griffin, S. T.; Rogers, R. D. *Ind. Eng. Chem. Res.* **2000**, *29*, 3596−3604. (c) Visser, A. E.; Swatloski, R. P.; Reichert, W. M.; Mayton, R.; Sheff, S.; Wiezbicki, A.; Davis, J. H.; Rogers, R. D. *Chem. Commun.* **2001**, 135−136.

(8) Naylor, A.; Wilson, P. D. In *Handbook of Solvent Extraction*; Lo, T. C., Baird, M. H. I., Hanson, C., Eds.; John Wiley & Sons: New York, 1983; p 783.

(9) (a) Gau, W. J.; Sun, I. W. *J. Electrochem. Soc.* **1996**, *143*, 170−174. (b) Gau, W. J.; Sun, I. W. *J. Electrochem. Soc.* **1996**, *143*, 914−919. (c) Tsuda, T.; Nohira, T.; Ito, Y. *Electrochim. Acta* **2001**, *46*, 1891−1897. (d) Matsumoto, K.; Tsuda, T.; Nohira, T.; Hagiwara, R.; Ito, Y.; Tamada, O. *Acta Crystallogr., Sect. C* **2002**, *8*, m186−m187. (e) Tsuda, T.; Nohira, T.; Ito, Y. *Electrochim. Acta* **2002**, *47*, 2817−2822. (f) Chaumont, A.; Wipff, G. *Phys. Chem. Chem. Phys.* **2003**, *5*, 3481−3488.

(10) Harmon, C. D.; Smith, W. H.; Costa, D. A. *Radiat. Phys. Chem.* **2001**, *60*, 157−159.

(11) (a) Jeapes, A. J.; Thied, R. C.; Seddon, K. R.; Pitner, W. R.; Rooney, D. W.; Hatter, J. E.; Welton, T. World Patent WO115175, 2001. (b) Thied, R. C.; Hatter, J. E.; Seddon, K. R.; Pitner, W. R.; Rooney, D. W.; Hebditch, D. World Patent WO113379, 2001. (c) Fields, M.; Thied, R. C.; Seddon, K. R.; Pitner, W. R.; Rooney, D. W. World Patent WO9914160, 1999. (d) Thied, R. C.; Seddon, K. R.; Pitner, W. R.; Rooney, D. W. World Patent WO9941752, 1999. (e) Fields, M.; Hutson, G. V.; Seddon, K. R.; Gordon, C. M. World Patent WO9806106, 1998.

(12) (a) Bradley, A. E.; Hatter, J. E.; Nieuwenhuyzen, M.; Pitner, W. R.; Seddon, K. R.; Thied, R. C. *Inorg. Chem.* **2002**, *41*, 1692−1694. (b) Allen, D.; Baston, G.; Bradley, A. E.; Gorman, T.; Haile, A.; Hamblett, I.; Hatter, J. E.; Healey, M. J. F.; Hodgson, B.; Lewin, R.; Lovell, K. V.; Newton, G. W. A.; Pitner, W. R.; Rooney, D. W.; Sanders, D.; Seddon, K. R.; Sims, H. E.; Thied, R. C. *Green Chem.* **2002**, *4*, 152−158. (c) Pitner, W. R.; Bradley, A. E.; Rooney, D. W.; Sanders, D.; Seddon, K. R.; Thied, R. C.; Hatter, J. E. In *Green Industrial Applications of Ionic Liquids*, Rogers, R. D., Seddon, K. R., Volkov, S.; Eds.; NATO Science Series II, Vol. 92; Kluwer Academic Publishers: Dordrecht, The Netherlands, 2002; pp 209−226,. (d) Baston, G. M. N.; Bradley, A. E.; Gorman, T.; Hamblett, I.; Hardacre, C.; Hatter, J. E.; Healy, M. J. F.; Hodgson, B.; Lewin, R.; Lovell, K. V.; Newton, G. W. A.; Nieuwenhuyzen, M.; Pitner, W. R.; Rooney, D. W.; Sanders, D.; Seddon, K. R.; Simms, H. E.; Thied, R. C. In *Ionic Liquids as Green Solvents: Progress and Prospects*; Rogers, R. D., Seddon, K. R., Eds; ACS Symposium Series 818; American Chemical Society: Washington, DC, 2002; pp 162−167.

(13) Weigel, F. In *The Chemistry of the Actinide Elements*; Katz, J. J., Seaborg, G. T., Moris, L. R., Eds.; Chapman and Hall: Bristol, U.K., 1986; p 169.

(14) (a) Wilkes, J. S.; Levisky, J. A.; Wilson, R. A.; Hussey, C. L. *Inorg. Chem.* **1982**, *21*, 1263−1264. (b) Seddon, K. R.; Stark, A.; Torres, M. J. *Pure Appl. Chem.* **2000**, *72*, 2275−2287.

**Table 1.** X-ray Experimental Crystal Data

| | **1** | **2** | **3** | **4**[a] |
|---|---|---|---|---|
| empirical formula | $C_{10}H_{18}N_8O_{14}U$ | $C_{14}H_{22}N_8O_{20}U_2$ | $C_{16}H_{26}N_8O_{20}U_2$ | $C_{18}H_{30}N_8O_{20}U_2$ |
| fw | 712.35 | 1098.46 | 1126.51 | 1154.56 |
| space group | $P\bar{1}$ | $P\bar{1}$ | $P2_1/c$ | $P2_1/n$ |
| unit cell dimens | | | | |
| *a*, Å; α, deg | 8.0385(15); 91.924(3) | 11.075(4); 102.167(9) | 15.405(3); 90 | 15.452(2); 90 |
| *b*, Å; *β*, deg | 8.3134(15); 100.692(3) | 15.077(4); 94.297(8) | 19.744(4); 106.629(4) | 20.354(3); 106.840(15) |
| *c*, Å; *γ*, deg | 8.6759(16); 109.428(3) | 29.599(8); 108.971(6) | 10.5297(18); 90 | 10.822(4); 90 |
| vol, Å$^3$; *Z* | 534.43(17); 1 | 4514(2); 6 | 3068.8(10); 4 | 3257.6(13); 4 |
| density(calcd), Mg m$^{-3}$ | 2.213 | 2.425 | 2.438 | 2.354 |
| cryst dimens (mm) | 0.45 × 0.18 × 0.16 | 0.48 × 0.18 × 0.08 | 0.26 × 0.23 × 0.06 | 0.51 × 0.33 × 0.09 |
| abs coeff, mm$^{-1}$ | 7.679 | 10.845 | 10.637 | 10.023 |
| *F*(000) | 338 | 3036 | 2088 | 2152 |
| *θ* range for data collection | 2−28 | 1.4−25 | 1.5−29 | 2−45 |
| no. of reflns collected | 5754 | 43704 | 25941 | 5100 |
| no. of independent reflns ($R_{int}$) | 2281 (0.0281) | 15825 (0.0826) | 7209 (0.0845) | 4033 |
| final *R* indices, R1 (wR2) | 0.0330 (0.0848) | 0.1066 (0.3377) | 0.0414 (0.1297) | 0.0584 (0.1459) |

| | **5** | **6**[b] | **7** | **8** |
|---|---|---|---|---|
| empirical formula | $C_{20}H_{34}N_8O_{20}U_2$ | $C_{32}H_{57}N_{11}O_{23}U_2$ | $C_{32}H_{62}N_8O_{14}U$ | $C_{52}H_{93}N_{13}O_{20}U_2$ |
| fw | 1182.61 | 1439.95 | 1020.93 | 1696.45 |
| space group | $P2_1/c$ | $P2_1/c$ | $P\bar{1}$ | $P\bar{1}$ |
| unit cell dimens | | | | |
| *a*, Å; α, deg | 10.6247(17); 90 | 14.722(3); 90 | 8.1071(7); 95.467(2) | 9.149(2); 94.643(4) |
| *b*, Å; *β*, deg | 19.020(3); 100.856(3) | 32631(7); 96.555(5) | 9.2880(8); 91.533(4) | 9.973(2); 96.437(4) |
| *c*, Å; *γ*, deg | 17.095(3); 90 | 10.587(2); 90 | 28.349(2); 93.733(2) | 24.330(6); 113.847(4) |
| vol, Å$^3$; *Z* | 3392.7(9); 4 | 5052.5(19); 4 | 2119.2(3); 2 | 1998.1(8); 1 |
| density(calcd), Mg m$^{-3}$ | 2.315 | 1.893 | 1.600 | 1.410 |
| cryst dimens (mm) | 0.32 × 0.10 × 0.10 | 0.20 × 0.10 × 0.06 | 0.28 × 0.26 × 0.12 | 0.52 × 0.20 × 0.16 |
| abs coeff, mm$^{-1}$ | 9.627 | 6.489 | 3.899 | 4.112 |
| *F*(000) | 2216 | 2776 | 1028 | 840 |
| *θ* range for data collection | 1.6−28.5 | 1.25−22.5 | 1.4−28.25 | 0.85−25 |
| no. of reflns collected | 37510 | 39166 | 17610 | 16142 |
| no. of independent reflns ($R_{int}$) | 7713 (0.0521) | 6604 (0.1723) | 9146 (0.0380) | 7012 (0.1166) |
| final *R* indices, R1 (wR2) | 0.0322 (0.0888) | 0.1506 (0.4463) | 0.0386 (0.1022) | 0.0937 (0.2840) |

[a] The crystal structure of **4** was previously published,[12a] and the experimental data are included here for comparison. [b] Crystals were small and of a poor quality, but connectivity has been established. The structure has been included because of the presence of an ionic liquid as a "solvent" of crystallization.

acid (1 g), and acetone (0.1 g). This mixture was heated to 70 °C for 2 h and allowed to cool. For $n = 1-6$, this procedure was found to result in the precipitation of a yellow solid which could be separated by filtration and recrystallized from ethanenitrile. For $n > 6$, cooling did not cause precipitation, and the formation of the solid salt was achieved by dissolving the reaction mixture in a minimum amount of ethanenitrile, addition of ethyl ethanoate, and cooling of the mixture.

$[C_4mim]_2[\{UO_2(NO_3)_2\}_2(\mu\text{-}C_2O_4)]$ was also generated using glyoxal as the source of the oxalate bridge. $[C_nmim][NO_3]$ (10 g), uranium(IV) nitrate hexahydrate (1 g), concentrated nitric acid (1 g), and glyoxal (0.1 g) were combined and heated to 70 °C for 2 h, leading to the formation of a yellow precipitate. Cell parameter determination using X-ray diffraction confirmed that the precipitate was $[C_4mim]_2[\{UO_2(NO_3)_2\}_2(\mu\text{-}C_2O_4)]$. The cell parameters for the precipitate generated from acetone or glyoxal were $a = 15.542(3)$ Å, $b = 20.354(3)$ Å, $c = 10.822(4)$ Å, and $\beta = 106.84(2)°$ and $a = 15.436(7)$ Å, $b = 20.391(9)$ Å, $c = 10.795(5)$ Å, and $\beta = 106.72(1)°$, respectively.

The oxidative dissolution of $UO_2$ was performed by reacting uranium(IV) dioxide (1 g, from BNFL) in the ionic liquid (10 g) with concentrated nitric acid (1 g, approximately 10% of the reaction volume) at 70 °C for 2 h either without added acetone or in the presence of 0.2 M acetone and allowed to cool. This led to the formation of bright yellow solutions of dioxouranium(VI) nitrate.

**Single-Crystal X-ray Crystallography.** Experimental parameters and crystal data are listed in Table 1. Data were collected on a Siemens P4 diffractometer using the XSCANS software with *ω* scans for **4**. For all other structures, a Bruker SMART diffractometer using the SAINT-NT software was used. A crystal was mounted onto the diffractometer at low temperature under dinitrogen at ca. 120 K. The structures were solved using direct methods with the SHELXTL program package, and the non-hydrogen atoms were refined with anisotropic thermal parameters. Hydrogen atom positions were added at idealized positions and refined using a riding model. Lorentz, polarization, and empirical absorption corrections were applied. The function minimized was $\sum[w(|F_o|^2 - |F_c|^2)]$ with reflection weights $w^{-1} = [\sigma^2|F_o|^2 + (g_1P)^2 + (g_2P)]$, where $P = [\max |F_o|^2 + 2|F_c|^2]/3$. Additional material available from the Cambridge Crystallographic Data Centre comprises relevant tables of atomic coordinates, bond lengths and angles, and thermal parameters (CCDC Nos. 224130−224136). All complexes (except **6**) produced by the method described above were prepared for X-ray crystallography by recrystallization of the precipitate from ethanenitrile. **6** was obtained directly from the ionic liquid.

**Extended X-ray Absorbance Fine Structure (EXAFS) Spectroscopy.** Data were collected at the Synchrotron Radiation Source in Daresbury, U.K., using station 9.2, at room temperature. The transmission detection mode was used with two ionization chambers filled with argon. The spectra were recorded at the uranium $L_{III}$ edge using a double-crystal Si(220) monochromator set at 50% harmonic rejection. A minimum of three scans per sample were required to obtain a sufficiently good signal-to-noise ratio. Scans were collected and averaged using EXCALIB, which was also used to convert raw data into energy vs absorption data. EXBROOK was used to remove the background. The analysis of the EXAFS spectra was performed using EXCURV98 on the raw data using the curved wave theory. Phase shifts were derived from ab initio

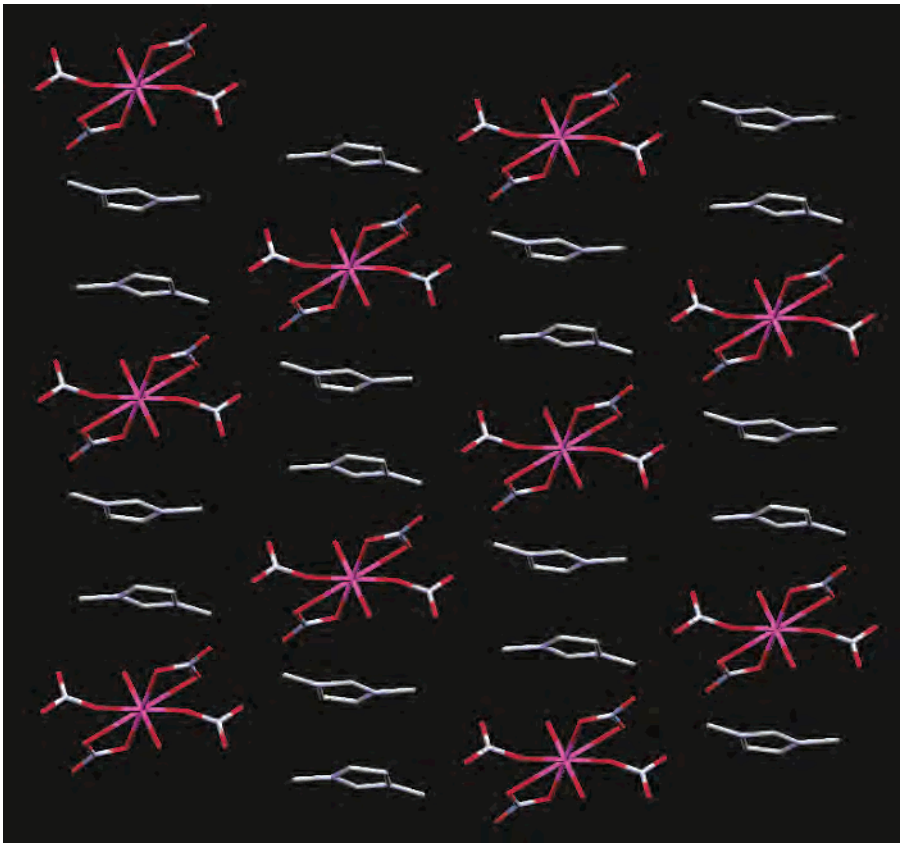

**Figure 1.** Illustration of the cation−anion columns in **1**, showing the cationic dimers with anions above and below. Hydrogen atoms have been omitted for clarity.

calculations using Hedin−Lundqvist exchange potentials and von Barth ground states. Multiple scattering was employed for the dioxouranium(VI) oxygens and the oxalate groups defined as individual units within the analysis package. During the fitting procedure for each of the complexes, the coordination numbers were fixed and the absorber−scatterer distances, Debye−Waller factors, and Fermi energy correction were refined using a least-squares refinement procedure. For the solutions containing a mixture of species, the coordination numbers were calculated to represent a particular ratio. Model structures used to obtain the starting position for the EXAFS analysis were obtained from X-ray structures of uranyl nitrate and **4**. The phase shifts were tested against measured solid samples of uranyl nitrate and **4** and compared with those of the X-ray structures. Monodentate nitrate structures were obtained from a survey of the Cambridge Crystollographic Database for similar complexes, for example, 2,4,6-trimethylpyridinium dinitratodioxo(2,4-pentanedionato-*O*,*O*′)uranium(VI) and 1,4,7,10,13,16-hexaoxacyclooctadecane diaquadinitratodioxouranium dihydrate. The solution data were measured using procedures described in detail elsewhere.[15]

**Electrochemical Analysis.** All electrochemical experiments were carried out with an EG&G PARC model 283 potentiostat/galvanostat connected to a PC through an IEEE-488 bus and controlled using EG&G Parc model 270/250 Research Electrochemistry version 4.23 software. Positive feedback *iR* compensation was employed to eliminate errors due to solution resistance. The electrochemical cell was constructed from materials purchased from Bioanalytical Systems, Inc. (BAS). The nonaqueous reference electrode was a silver wire immersed in a glass tube containing a 0.100 mol $L^{-1}$ solution of $AgNO_3$ in the $[C_n mim][NO_3]$ ionic liquid separated from the bulk solution by a Vycor plug. All potentials reported are referenced against the $AgNO_3$/Ag couple. The counter electrode was a platinum coil immersed directly in the bulk solution. The working electrode was a glassy carbon disk ($A = 7.07 \times 10^{-2}$ $cm^2$). The solution was held in a glass vial fitted with a Teflon cap with holes for the electrodes and a gas line. All work was carried out under a dry dinitrogen atmosphere, and dinitrogen was bubbled through the solution prior to performanc of electrochemical experiments. All electrochemical experiments were carried out at 40 °C with a scan rate of 50 mV $s^{-1}$. The nitrogen used was 99.99% (BOC) and was dried prior to use. The ionic liquids used in the electrolysis had a $Cl^-$ content <20 ppm as measured by a chloride-selective electrode, and all organic impurities were below the NMR detection limit.[14b] Prior to dissolution of **4**, the ionic liquid was dried at 60 °C overnight under high vacuum. Typically a residual water content of <1 wt % as measured by Karl Fischer analysis was obtained after this procedure.

## Results

**X-ray Crystallography. 1,3-Dimethylimidazolium Bis(nitrato-*O*,*O*)bis(nitrato-*O*)dioxouranate(VI) (1).** The asymmetric unit of $[C_1mim]_2[UO_2(NO_3)_4]$ consists of one imidazolium cation and a half-anion located on an inversion center. The cations and anions are arranged into columns aligned in the (011) direction (Figure 1). These consist of alternating regions of anions and cations. The imidazolium cations form a dimeric motif via $\pi\cdots\pi$ interactions. The dimeric motif has uranate(VI) anions above and below it with the oxygen atoms directed toward the C2 position of the imidazolium cations at an O···C distance of 2.85 Å. These

(15) Hamill, N. A.; Hardacre, C.; McMath, S. E. J. *Green Chem.* **2002**, *4*, 139−142.

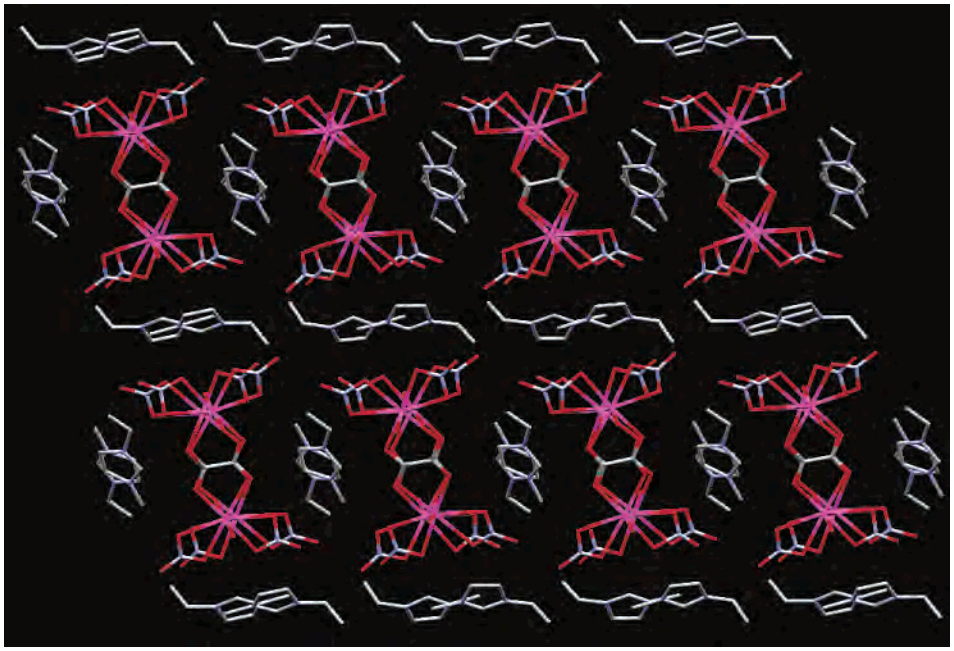

**Figure 2.** Illustration of the cation and anion columns in **2** showing the template effect of the anions. Hydrogen atoms have been omitted for clarity.

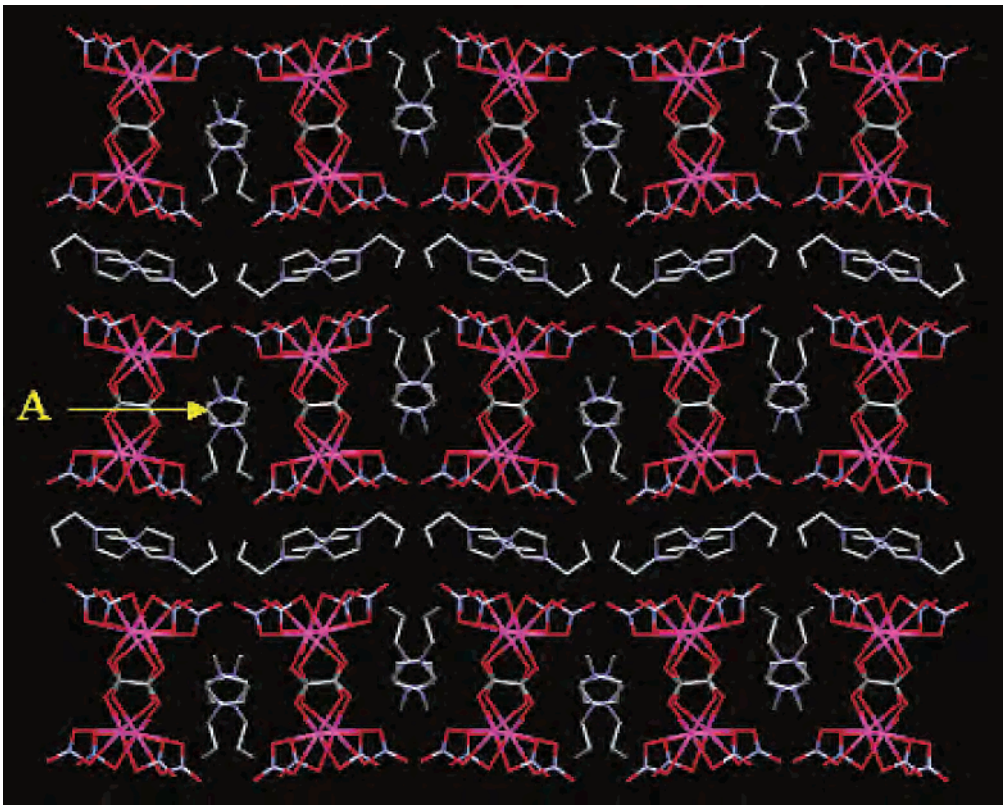


**Figure 3.** Illustration of the cation−anion arrangement in **3** showing the cations surrounding the anion columns. Hydrogen atoms have been omitted for clarity.

columns of cations and anions are arranged into a three-dimensional network via C−H···O hydrogen bonds.

**1-Ethyl-3-methylimidazolium $\mu_4$-(*O*,*O*,*O*′,*O*′-Ethane-1,2-dioato)bis[bis(nitrato-*O*,*O*)dioxouranate(VI)] (2)**. The asymmetric unit contains four unique anions, two of which are located about inversion centers, and six unique cations (Figure 2). The large number of cations and anions in the asymmetric unit is probably the result of the flexibility of the ethyl moiety, giving the following C2−N1−C6−C7 torsion angles: 114.1°, 102.8°, 96.9°, 166.5°, 175.1°, and 169.6°. The cations are arranged in methyl C−H···$\pi$/$\pi$···$\pi$ hydrogen-bonded columns along the (001) direction. The anions are also aligned in columns, and they act as a template for the columns of cations which surround them.

**1-Propyl-3-methylimidazolium $\mu_4$-(*O*,*O*,*O*′,*O*′-ethane-1,2-dioato)bis[bis(nitrato-*O*,*O*)-dioxouranate(VI)] (3)**.

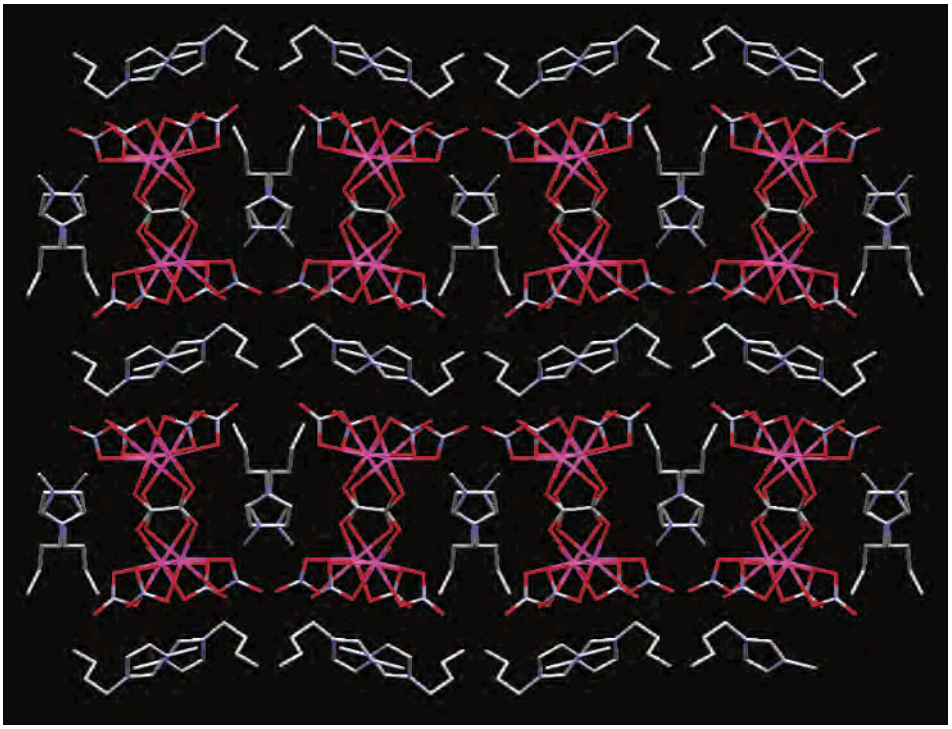

**Figure 4.** Illustration of the cation−anion arrangement in **4** showing the cations surrounding the anion columns. Hydrogen atoms have been omitted for clarity.

The asymmetric unit contains two unique cations and two unique anions (Figure 3). The anions are positioned such that they lie about centers of inversion and consist of two $\{UO_2(NO_3)_2\}$ units, bridged by an oxalate anion. The propyl chains of the imidazolium cations adopt two conformations: the first is almost coplanar with the imidazolium ring, with a C2−N1−C5−C6 torsion angle of −130.6° (shown as A in Figure 3); the second is close to perpendicular to the imidazolium ring, with a C2−N1−C5−C6 torsion angle of −115.0°. The anions are arranged into columns with the two conformationally different cations "encapsulating" the anionic columns aligned in the (001) direction.

**1-Butyl-3-methylimidazolium $\mu_4$-(*O*,*O*,*O*′,*O*′-Ethane-1,2-dioato)bis[bis(nitrato-*O*,*O*)dioxouranate(VI)] (4)**. X-ray analysis of **4** shows the unit cell contains four $[C_4mim]^+$ cations and two independent $[\{UO_2(NO_3)_2\}_2(\mu\text{-}C_2O_4)]^{2-}$ anions, both of which are located about inversion centers (Figure 4). The $[C_4mim]^+$ cations are arranged such that they produce large channels in which the anions are located. Thus, as in **2** and **3** above, the anions effectively act as a template for the cations. The flexibility of the alkyl chains on the cations is illustrated by the differences in the C2−N1−C6−C7 torsion angles for the butyl chain at 104.7° and 129.1°.

**1-Pentyl-3-methylimidazolium $\mu_4$-(*O*,*O*,*O*′,*O*′-Ethane-1,2-dioato)bis[bis(nitrato-*O*,*O*)dioxouranate(VI)] (5)**. As in **3** and **4** above, the asymmetric unit contains two unique anions located about inversion centers and two unique cations, with the alkyl chains adopting either a linear or a bent orientation with respect to the imidazolium ring (C2−N1−C6−C7 torsion angles of 89.7° and −85.3°, respectively). The anions still act as a template for the cations (Figure 5), resulting in columns of anions surrounded by columns of cations aligned in the (100) direction. However,

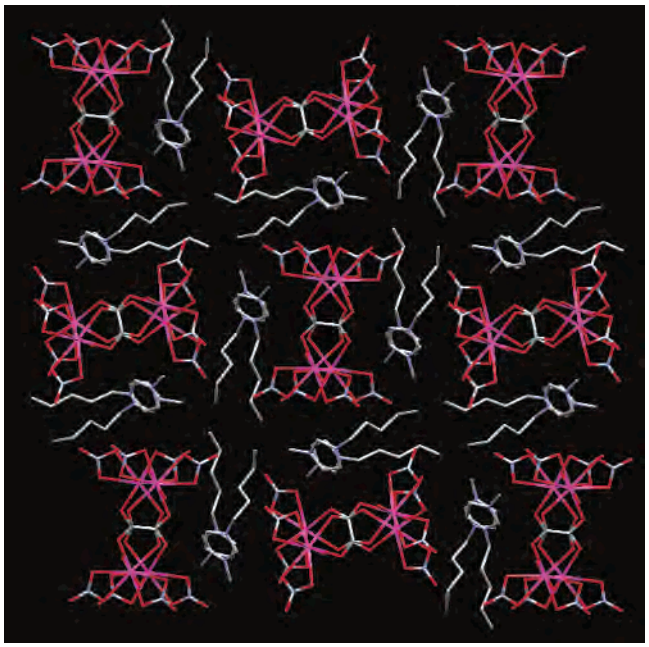

**Figure 5.** Illustration of the cation−anion arrangement in **5** showing the cations surrounding the anion columns and the orthogonal relationship between adjacent anion columns. Hydrogen atoms have been omitted for clarity.

the relative orientation of the anion columns to each other is different from those in **2**, **3**, and **4** above; in **5**, the adjacent columns are rotated through 90° from one another.

**1-Hexyl-3-methylimidazolium $\mu_4$-(*O*,*O*,*O*′,*O*′-Ethane-1,2-dioato)bis[bis(nitrato-*O*,*O*)-dioxouranate(VI)]/1-Hexyl-3-methylimidazolium Nitrate (1/1) (6)**. The asymmetric unit contains one oxalate-bridged dinuclear anion, one nitrate anion, and three unique cations, one of which is disordered

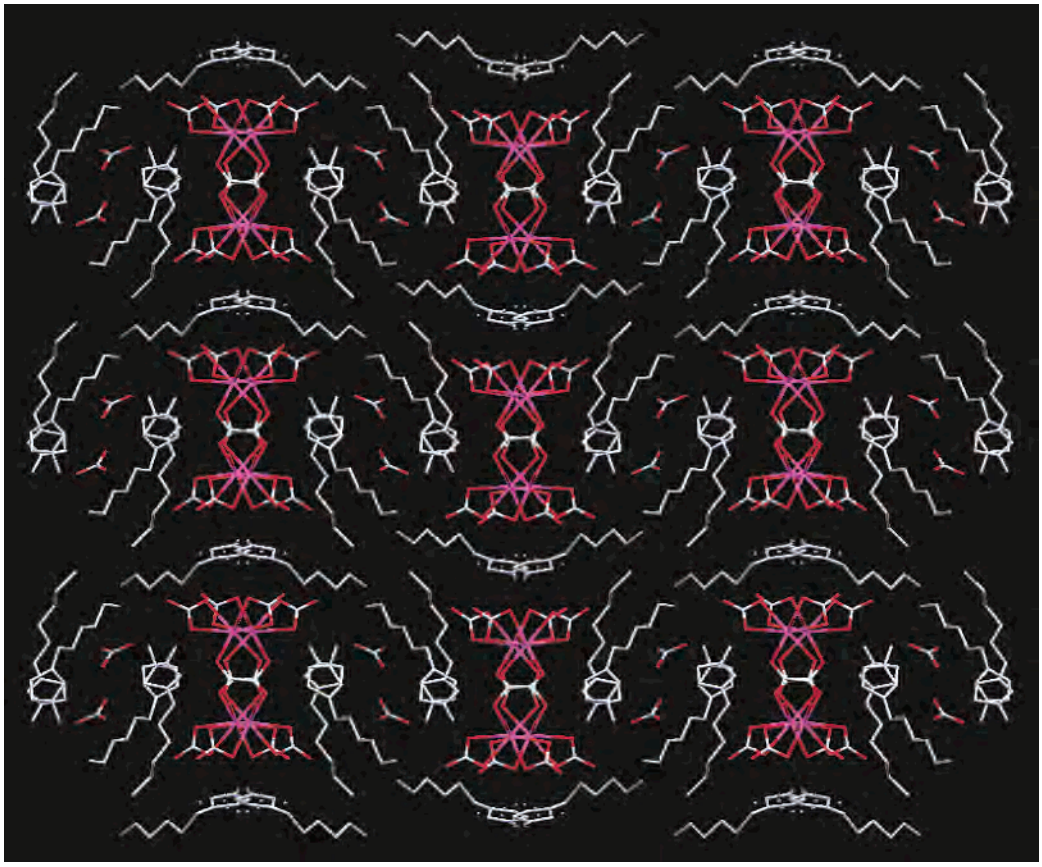

**Figure 6.** Illustration of the cation−anion arrangement in **6** showing the cations and solvate ionic liquid surrounding the anion columns. Hydrogen atoms have been omitted for clarity.

(Figure 6). The dimers are aligned in columns in the (001) direction, with adjacent columns being parallel to each other, unlike the orthogonal relationship seen in **5**. The anions still act as templates for the cation, but because of the length of the hexyl chains, the structure has crystallized as a solvate containing the 1-hexyl-3-methylimidazolium nitrate ionic liquid. The general features of the structure are similar to those of salts **2**−**4**.

**1-Dodecyl-3-methylimidazolium Bis(nitrato-*O*)bis(nitrato-*O*,*O*)dioxouranate(VI)] (7)**. The asymmetric unit contains one anion and two cations. The anions are associated with the imidazolium headgroups of the cations, with the alkyl chains extending in a linear fashion away from this region. Adjacent alkyl chains are directed toward one another, forming an interdigitated bilayer containing "charged" regions alternating with "neutral" alkyl regions which are typical for long-chain imidazolium salts,[16] Figure 7. The two cations do not show the same variation in the conformations of the alkyl chains (as seen in the shorter chains of **1**−**6**); in **7**, the chains are linear.

**1-Hexadecyl-3-methylimidazolium $\mu_4$-(*O*,*O*,*O*′,*O*′-Ethane-1,2-dioato)bis[bis(nitrato-*O*,*O*)dioxouranate(VI)]/Ethanenitrile (1/6) (8)**. The asymmetric unit contains one unique anion which is located about an inversion center, one cation, and three ethanenitrile molecules, two of which are disordered. The cations and anions are arranged such that the anions are associated into columns along the (001) direction, with the imidazolium headgroups hydrogen bonding to these columns. The alkyl chains extend away from these charged regions, forming an interdigitated bilayer similar to that observed in **7**. This arrangement leads to large channel-like "voids" in this lattice, with the closest contact between alkyl chains being 8.0 Å, Figure 8. The voids are filled with ethanenitrile solvent molecules, which are disordered and thus adopt random positions throughout the channels.

**EXAFS Spectroscopy**. Figure 9 shows the EXAFS data and *pseudo*radial distribution functions obtained from solutions of $UO_2(NO_3)_2 \cdot 6H_2O$ and **4** dissolved in $[C_4mim][NO_3]$ at room temperature and the reaction solution following the oxidative dissolution of $UO_2$ in $[C_4mim][NO_3]$, without added acetone and in the presence of 0.2 M acetone. The parameters used to model the experimental data are summarized in Table 2. On dissolution of **4** in $[C_4mim][NO_3]$, the EXAFS spectrum indicates that the oxalate dinuclear species remains intact in solution and the hydrated dioxouranium(VI) cation is not formed. The analysis also shows that the $\eta^2$-$NO_3$ groups are not displaced by water. This may be compared with the in situ formation of dioxouranium(VI) oxalate species in water. Vallet et al. showed that, on

(16) (a) Bradley, A. E.; Hardacre, C.; Holbrey, J. D.; Johnston, S.; McMath, S. E. J.; Nieuwenhuyzen, M. *Chem. Mater.* **2002**, *14*, 629−635. (b) Gordon, C. M.; Holbrey, J. D.; Kennedy, A. R.; Seddon, K. R. *J. Mater. Chem.* **1998**, *8*, 2627−2636. (c) Hardacre, C.; Holbrey, J. D.; McCormac, P. B.; McMath, S. E. J.; Nieuwenhuyzen, M.; Seddon, K. R. *J. Mater. Chem.* **2001**, *11*, 346−350. (d) Bowlas, C. J.; Bruce, D. W.; Seddon, K. R. *J. Chem. Soc., Chem. Commun.* **1996**, 1625−1626.

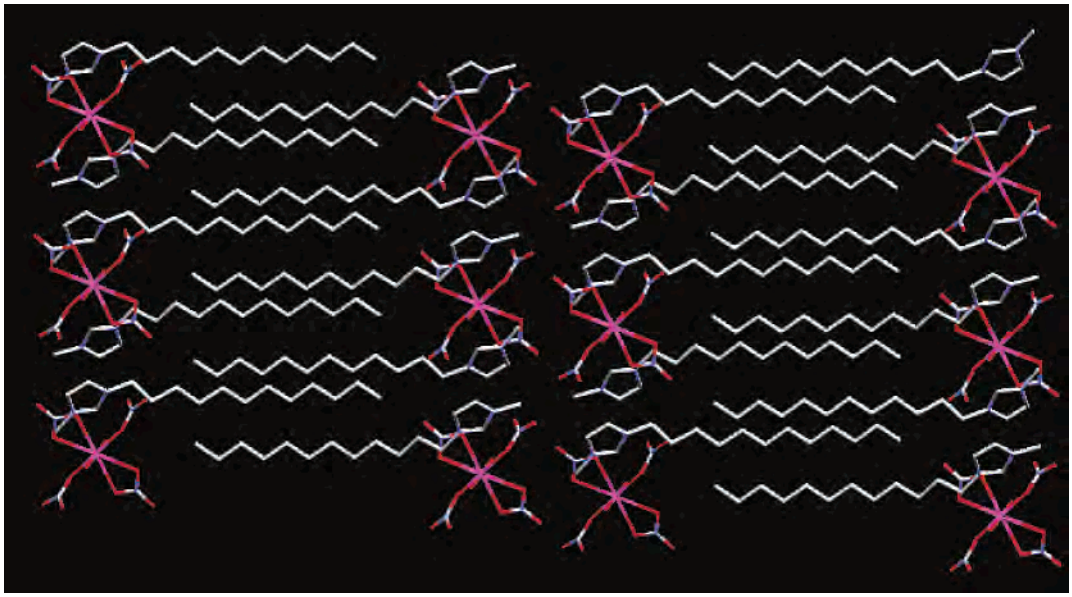

**Figure 7.** Illustration of the cation−anion arrangement in **7** showing the anions associated with cationic headgroups, and with the alkyl chains interdigitated. Hydrogen atoms have been omitted for clarity.

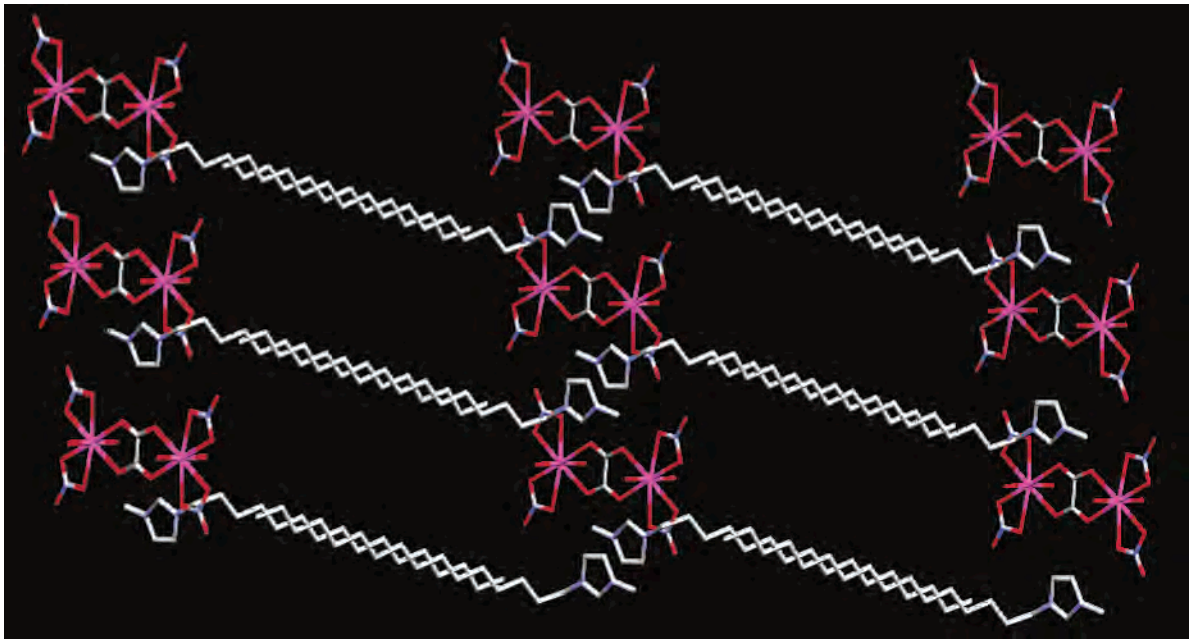

**Figure 8.** Illustration of the cation−anion arrangement in **8** showing the anions associated with cationic headgroups and channels between the alkyl chain regions. The MeCN molecules have been omitted for clarity.

dissolution of uranyl nitrate in the presence of sodium oxalate, $[UO_2(oxalate)_2(H_2O)]^{2-}$ was formed.[17] There are two main multiple scattering pathways that contribute significantly to the final fit for the EXAFS data: one derived from the dioxouranium(VI) unit and the other from the oxalate unit, in agreement with other studies.[17,18] In the pseudoradial distribution functions shown in Figure 9, the largest peak can be attributed to the dioxouranium(VI) shell, and the second set of peaks is a convolution of the shells associated with the nitrate and oxalate ligands. The U−U distance present in **4** is not seen in the EXAFS data due to the long length of the U···U distance, 6.3 Å. Where peaks have been noted in other dinuclear structures, the U···U distances are below 4 Å.[18]

Comparing the EXAFS data for the pure dinuclear oxalate and mononuclear nitrate complexes dissolved in the ionic liquid with those of the solutions obtained after dissolution of $UO_2$ in $[C_4mim][NO_3]$ indicates that a mixture of species is present. Furthermore, the addition of acetone had little effect on the EXAFS data. For both solutions, following dissolution of $UO_2$, the best fit was obtained with a 15/85 mononuclear nitrate/dinuclear oxalate mole ratio present in solution. The error in the proportion of nitrate monomer present is high (±10 mol %) due to the shallow-

(17) Vallet, V.; Moll, H.; Wahlgren, U.; Szabó, Z.; Grenthe, I. *Inorg. Chem.* **2003**, *42*, 1982−1993.

(18) Barnes, C. E.; Shin, Y.; Saengkerdsub, S.; Dai, S. *Inorg. Chem.* **2000**, *39*, 862−864.

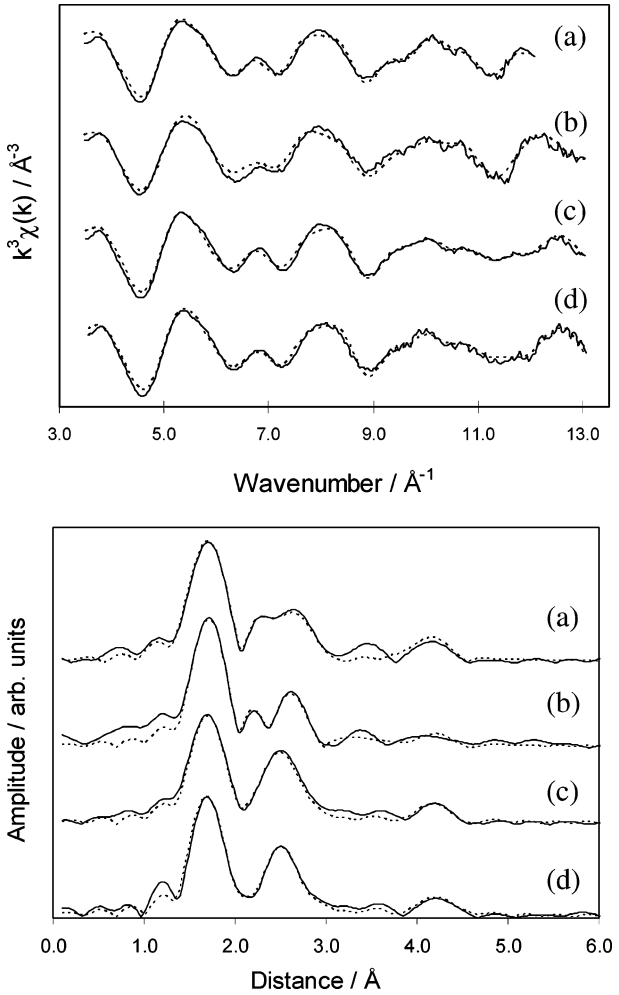


**Figure 9.** Comparison of the experimental (solid line) and fitted (dashed line) EXAFS spectra (upper) and pseudoradial distribution (lower) functions from (a) $UO_2(NO_3)_2{\cdot}6H_2O$ and (b) $[C_4mim]_2[\{UO_2(NO_3)_2\}_2(\mu_4\text{-}C_2O_4)]$, **4**, dissolved in $[C_4mim][NO_3]$ and following $UO_2$ dissolution in $[C_4mim][NO_3]$ (c) in the absence of acetone and (d) in the presence of 0.2 M acetone.

ness of the minimum found in the fit on varying the composition.

Clearly good agreement between the EXAFS spectrum and that of the hydrated dioxouranium(VI) nitrate species is obtained as observed in Figure 9a. However, there are a number of possible structural arrangements on dissolution of $UO_2(NO_3)_2{\cdot}6H_2O$ in the nitrate ionic liquid involving monodentate nitrate coordination, namely, $[UO_2(\eta^2\text{-}NO_3)_2(\eta^1\text{-}NO_3)(H_2O)]^-$ and $[UO_2(\eta^2\text{-}NO_3)_2(\eta^1\text{-}NO_3)_2]^{2-}$. Using the $\chi^2$ statistical tests, the EXAFS spectrum was also fitted using one monodentate nitrate and two monodentate nitrate ligands with fit factors of 16.8% ($\chi^2 = 1.105$) and 17.6% ($\chi^2 = 1.213$), respectively. This may be compared with a fully hydrated coordination with a fit factor of 18.1% ($\chi^2 = 1.135$). From the analysis, it is clear that despite the larger number of parameters, and consequently the better fit, $[UO_2(\eta^2\text{-}NO_3)_2(\eta^1\text{-}NO_3)_2]^{2-}$ is unlikely to be present due to the higher $\chi^2$ value. Although the $\chi^2$ values are similar, the analysis would also suggest that the $[UO_2(\eta^2\text{-}NO_3)_2(\eta^1\text{-}NO_3)(H_2O)]^-$ species may be formed, i.e., an ionic species. Analogous analysis was performed on the solutions following $UO_2$ dissolution. For each species, i.e., both hydrated and those containing monodentate nitrate, the best fits were obtained using a 15/85 mononuclear nitrate/dinuclear oxalate mole ratio as described above. At this ratio, the fit factors were found to be 19.2% ($\chi^2 = 1.068$) for $[UO_2(NO_3)_2(H_2O)_2]$, 18.8% ($\chi^2 = 1.110$) for $[UO_2(\eta^2\text{-}NO_3)_2(\eta^1\text{-}NO_3)(H_2O)]^-$, and 18.5% ($\chi^2 = 1.060$) for $[UO_2(\eta^2\text{-}NO_3)_2(\eta^1\text{-}NO_3)_2]^{2-}$, indicating that the latter is most consistent with the EXAFS spectrum. If the same species is present in all three systems containing the nitrate monomer, the $\chi^2$ analysis would suggest that the neutral species is present, as shown in Figure 9 and Table 2. However, it is quite likely that a range of neutral and anionic species are present in each case, and that the solution contains an equilibrium mixture. Unfortunately, from the quality of the EXAFS data obtained, it is not possible to assign definitively the species or the ratio present.

**Electrochemistry.** The electrochemical behavior of 0.1 M **4** in $[C_4mim][NO_3]$ was investigated using cyclic voltammetry. A typical cyclic voltammogram is shown in Figure 10. The voltammogram is characterized by a broad irreversible reduction wave with a peak around −0.9 V. The broad oxidation wave with a peak around −0.1 V is associated with the reduction wave, but its relatively small amplitude indicates the irreversible nature of the reduction. The ionic liquid does not show any features in this region and has a cathodic limit of −2.4 V and an anodic limit of +1.5 V with respect to a $Ag^+/Ag$ couple; therefore, these features are thought to be associated with **4**.

Exhaustive electrolysis was repeatedly carried out at a glassy carbon flag working electrode ($A \approx 1$ cm$^2$) in an attempt to isolate the product. For constant potential electrolysis, the potential of the working electrode was held at a suitable negative potential (∼−1.2 V) to bring about reduction of the $[C_4mim]_2[\{UO_2(NO_3)_2\}_2(\mu_4\text{-}C_2O_4)]$. This led to passivation of the electrode by a thin film of a brown powder. To prevent passivation of the electrode surface, electrolysis was carried out at −1.2 V while the potential was periodically pulsed to +1 V using a square-wave potential program. A typical potential program used during electrolysis consisted of holding the potential at −1.2 V for 59.9 s and at +1 V for 0.1 s in a continuous loop. Over time, the electrolysis solution changed from bright yellow to dark brown. Various attempts to isolate a product by filtration and solvent extraction were unsuccessful. However, the electrochemical reduction of **4** is a two-electron metal-centered reduction of uranium(VI) to uranium(IV), which is consistent with formation of a $UO_2$-type species.

## Discussion

The mixture postulated from the EXAFS results is consistent with UV−vis and IR measurements following oxidative dissolution of uranium(IV) oxide in the ionic liquid. The UV−vis spectrum of the yellow solution with a structured absorbance band at 415 nm (Figure 11) confirmed that uranium(VI) was present. The UV−vis spectrum is consistent with a uranium(VI) surrounded by six oxygens in the plane; however, more detailed analysis is ongoing to ascertain the speciation of the uranium. Infrared spectra of the liquid showed a fingerprint pattern in the 1000−1500

**Table 2.** Structural Parameters from the Fitted EXAFS Spectra for $UO_2(NO_3)_2 \cdot 6H_2O$ and **4** Dissolved in $[C_4mim][NO_3]$ and Following $UO_2$ Dissolution in $[C_4mim][NO_3]$ in the Absence of Acetone and in the Presence of 0.2 M Acetone[a]

| solution | atom | distance, Å | coordination no. | Debye−Waller factor, Å$^2$ | fit factor, % |
|---|---|---|---|---|---|
| $UO_2(NO_3)_2 \cdot 6H_2O/[C_4mim][NO_3]$ | O (U=O) | 1.75 | 2.0 | 0.005 | 18.1 |
| | O ($H_2O$) | 2.34 | 2.0 | 0.014 | |
| | O ($NO_3$) | 2.51 | 4.0 | 0.013 | |
| | N ($NO_3$) | 2.96 | 2.0 | 0.005 | |
| **4**/$[C_4mim][NO_3]$ | O (U=O) | 1.76 | 2.0 | 0.004 | 25.6 |
| | O ($NO_3$) | 2.52 | 4.0 | 0.014 | |
| | N ($NO_3$) | 2.89 | 2.0 | 0.001 | |
| | O (Ox) | 2.32 | 2.0 | 0.009 | |
| | C (Ox) | 3.06 | 2.0 | 0.001 | |
| $UO_2/[C_4mim][NO_3]$ without acetone | O (U=O) | 1.75 | 2.0 | 0.007 | 19.2 |
| | O ($H_2O$) | 2.33 | 0.3 | 0.017 | |
| | O ($NO_3$) | 2.49 | 4.0 | 0.009 | |
| | N ($NO_3$) | 2.95 | 2.0 | 0.006 | |
| | O ($NO_3$) | 4.15 | 2.0 | 0.013 | |
| | O (Ox) | 2.33 | 1.7 | 0.019 | |
| | C (Ox) | 3.23 | 1.7 | 0.050 | |
| | O (Ox) | 4.53 | 1.7 | 0.015 | |
| $UO_2/[C_4mim][NO_3]$ with 0.2 M acetone | O (U=O) | 1.75 | 2.0 | 0.006 | 19.2 |
| | O ($H_2O$) | 2.36 | 0.3 | 0.026 | |
| | O ($NO_3$) | 2.47 | 4.0 | 0.007 | |
| | N ($NO_3$) | 2.95 | 2.0 | 0.005 | |
| | O ($NO_3$) | 4.15 | 2.0 | 0.013 | |
| | O (Ox) | 2.28 | 1.7 | 0.011 | |
| | C (Ox) | 3.28 | 1.7 | 0.050 | |
| | O (Ox) | 4.55 | 1.7 | 0.005 | |

[a] Ox denotes oxalate, U=O denotes axial dioxouranium(VI) oxygens. The errors in the distances and Debye−Waller factors are estimated as ±1.5% and ±20%, respectively.

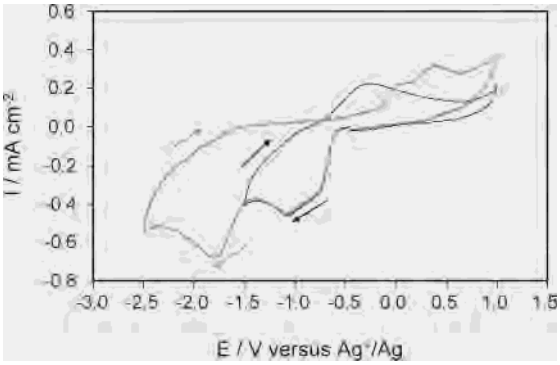


**Figure 10.** Cyclic voltammogram (scan rate 50 mV $s^{-1}$) of 0.1 M $[C_4mim]_2[\{UO_2(NO_3)_2\}_2(\mu_4\text{-}C_2O_4)]$ in $[C_4mim][NO_3]$, recorded at a glassy carbon electrode at 40 °C. The black line shows the first sweep, and the gray line shows the second sweep.

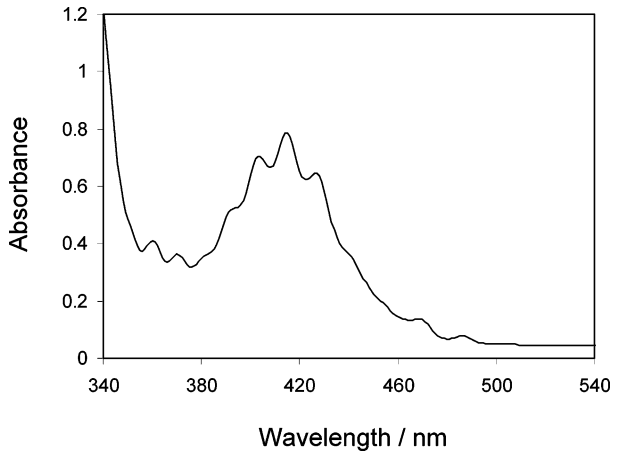


**Figure 11.** UV−vis following $UO_2$ oxidative dissolution in $[C_4mim][NO_3]$ using nitric acid.

$cm^{-1}$ region identical to that of **1**, which is assigned to tetradentate oxalate C−O stretching.

In our paper, we postulated[12a] that acetone in the reaction system may serve as the precursor to the oxalato-bridging species in the complex. However, it is clear from the solution-phase EXAFS results that, in both the presence and absence of added acetone, the same species are found in solution. Rogers et al.[19] reported the preparation of the anion $[\{UO_2(NO_3)_2\}_2(\mu\text{-}C_2O_4)]^-$ by heating dioxouranium(VI) sulfate trihydrate with concentrated nitric acid and a crown ether. The oxalate species was attributed to impurities in the nitric acid, as a variety of acids were used and the bridging oxalate anion was only noted when the complexes were prepared with nitric acid. Glyoxal is a starting material in the preparation of imidazole, which is required for the synthesis of imidazolium-based ionic liquids, and it has been noted that the oxidation of alcohols with concentrated nitric acid results in a variety of species including oxalate.[20] A test experiment replacing acetone with glyoxal confirmed that this could also be a source of the oxalate species. It is therefore possible that organic impurities in either the nitric acid or ionic liquid are oxidized to the oxalate ligand, which is trapped between two dioxouranium(VI) nitrate units.

The crystal structures of compounds **1**−**8** show a complicated and unpredictable behavior, with the majority exhibiting the formation of an oxalate complex. Examination of all the oxalate dimeric anions reported herein shows no significant structural changes as the alkyl length of the cation increases. These structures are consistent with previously

(19) Rogers, R. D.; Bond, A. H.; Hipple, W. G.; Rollins, A. N.; Henry, R. F. *Inorg. Chem.* **1991**, *30*, 2671−2679.

(20) (a) Behrend, R.; Schmitz, J. *Chem. Ber.* **1893**, *26*, 626. (b) Apetz, H.; Hell, C. *Chem. Ber.* **1894**, *27*, 933.

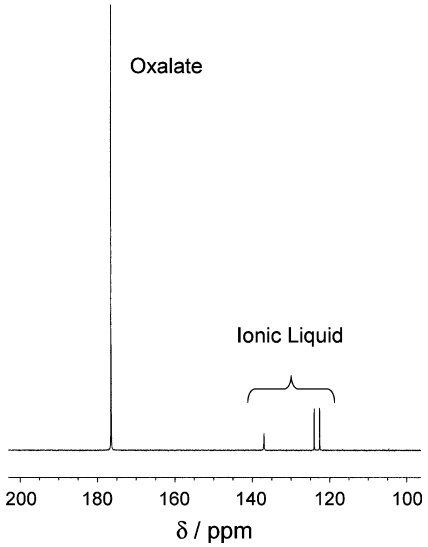


**Figure 12.** $^{13}C$ NMR following $UO_2$ oxidative dissolution in $[C_4mim][NO_3]$ using nitric acid in the presence of 0.2 M $(^{13}CH_3)_2CO$.

reported structures by Bradley et al.[12] and Rogers et al.[19] Only salts **1** and **7** have been characterized as 1,3-dialkylimidazolium bis(nitrato-*O*)bis(nitrato-*O*,*O*)dioxouranate(VI). To explain why **1** and **7** precipitate preferentially from the $[C_1mim]^+$ and $[C_{12}mim]^+$ ionic liquids, respectively, we need to recall that the EXAFS data from the $[C_4mim]^+$ ionic liquid showed a mixture of mononuclear and dinuclear anions; thus, both species can coexist in solution. This presence of the oxalate species has been confirmed for all the $[C_nmim]^+$ ionic liquids by NMR spectroscopy. For example, in the $^{13}C$ NMR spectra following the oxidation of uranium(IV) oxide by nitric acid in $[C_4mim][NO_3]$, a singlet peak at 177 ppm arising from the oxalate carbon atom is observed. This feature increases in intensity when the oxidation is carried out in the presence of either $(CH_3)_2{}^{13}CO$ or $(^{13}CH_3)_2CO$ (from Aldrich) (Figure 12). The differences in each of the crystals formed are therefore due to preferential precipitation of either the oxalate dimeric or nitrate monomer species.

For **1**, preferential crystallization of the nitrate-containing anions is probably due to the relative sizes of the cations and anions; i.e., the oxalate dimer anion is very large with respect to the $[C_1mim]^+$. Due to "packing" considerations, these anions remain in the melt while the smaller nitrate monomer anions are able to precipitate from the solution and form **1**. However, this does not explain the precipitation of **7**, where it is probable that 1-dodecyl-3-methylimidazolium $\mu_4$-(*O*,*O*,*O*′,*O*′-ethane-1,2-dioato)bis[bis(nitrato-*O*,*O*)dioxouranate(VI)] is a liquid at room temperature, whereas the nitrate monomer salt is a solid. For $n = 8-12$, the larger size of the dinuclear anion, compared with the mononuclear species, forces the chains apart, reducing the van der Waals interactions, and the salt is a liquid at room temperature. For $n = 16$ the molecular mass is sufficiently high for the solid dinuclear salt to form without the need for strong alkyl−alkyl interactions.

Salts **2**−**6** and **8** all contain $[\{UO_2(NO_3)_2\}_2(\mu_4\text{-}C_2O_4)]^{2-}$, and the packing of the anions in **2**−**5** results in columns of anions within the lattice. The differences arise as a result of the packing of the cations. In **2**, the cations are arranged such that the ethyl moiety alternates left to right throughout the lattice, Figure 2. This allows the methyl groups and the imidazolium rings to form C−H···$\pi$/$\pi$···$\pi$ hydrogen-bonded columns in the (001) direction, and the anions act as a template for the surrounding cations. In **3** and **4**, however, the cations that lie between the anions are aligned in the same direction. This orientation does not inhibit the cations from forming inter-ring interactions, but it does prevent any contribution from methyl C−H···$\pi$ interactions. Those that are at the "end" of the anions are still aligned opposite one another, and still form C−H···$\pi$/$\pi$···$\pi$ hydrogen-bonded columns. In **5**, none of the cationic columns show an alternating arrangement of the 1-alkyl chain with respect to the column, Figure 5. In fact, the 1-alkyl chains of adjacent columns are directed toward one another, giving alternating ionic and aliphatic regions within the lattice although there is no alkyl chain interdigitation.

The structure of **6** is unusual in that it is a cocrystal of the $[C_6mim]_2[\{UO_2(NO_3)_2\}_2(\mu_4\text{-}C_2O_4)]$ and the $[C_6mim][NO_3]$ ionic liquid. The incorporation of ionic liquids in crystal lattices is very rare, and there is only one other known example.[21] The cocrystallization is probably due to the length of the alkyl chains on the cations. These are not long enough to be able to form an interdigitated structure as in **7**. To overcome this, the nitrate ionic liquid solvent cocrystallizes with the dioxouranium(VI) salt.

In **8**, the hydrocarbon chains are long enough to form an interdigitated structure, with the anions associated with the headgroups. The relative sizes of the cationic headgroup and the larger size of the anions lead to "channels" between cationic layers. Crystals of **8**, unlike **6**, were not obtained directly from the ionic liquid, and were recrystallized from ethanenitrile: thus, the channels are filled with ethanenitrile molecules.

Electrochemical processes have been considered in the processing of spent nuclear fuel. The United States has designed their Integral Fast Reactor (IFR) Program to include a pyrochemical fuel recycling process.[22] In the Argonne National Laboratory (ANL) lithium process, declad oxide fuel is dissolved in a LiCl/KCl eutectic at 773 K. The oxides are reduced to metals in the presence of lithium metal. Uranium is then purified through an electrorefining process where the fuel is oxidized at an anode and purified uranium is deposited at a cathode. More noble metals than uranium, i.e., those having a more positive standard potential, remain at the anode, while less noble metals, i.e., those having a more negative standard potential, remain in the eutectic salt. A similar process being developed by the Research Institute of Atomic Reactors (RIAR) in Dimitrovgrad, Russia, operates in a NaCl/KCl melt at 1000 K.[23] In this process, oxide fuel is oxidatively dissolved using chlorine and oxygen gases. The uranium is then recovered as $UO_2$ through electrochemical reduction at a carbon cathode. This procedure works in

(21) Holbery, J. D.; Nieuwenhuyzen, M.; Seddon, K. R. Unpublished results.
(22) Laidler, J. J.; Battles, J. E.; Miller, W. E.; Ackerman, J. P.; Carls, E. L. *Prog. Nucl. Energy* **1997**, *31*, 131.

the processes described above due to the temperatures utilized. $UO_2$ is a conductor at 1000 K, whereas recovery of uranium using the ionic liquid process described herein is problematic because of the process operating temperature range, 298−400 K. $UO_2$ is an insulator at these temperatures, which makes electrochemical separation of uranium by reduction from $UO_2^{2+}$ to $UO_2$ much more difficult. As described above, without the constant refreshing of the electrode surface to remove the passivating film of $UO_2$, the current decreases to zero and the process stalls.

In conclusion, we have shown that the formation of 1-alkyl-3-methylimidazolium salts of the dinuclear $\mu_4$-(*O*,*O*,*O*′,*O*′-ethane-1,2-dioato)bis[bis(nitrato-*O*,*O*)dioxouranate(VI)] anion is general for a range of alkyl groups. In addition, during the oxidative dissolution of $UO_2$ in $[C_4mim][NO_3]$, similar uranium speciation is found whether acetone is added to the ionic liquid or not. The EXAFS data show clearly a mixture of complexes present and are consistent with a 15/85 mole ratio of a mononuclear nitrate complex/dinuclear oxalate complex. The exact structures of the complexes could not be unambiguously identified from the EXAFS data.

**Acknowledgment.** We thank BNFL for financial support (A.E.B, W.R.P., and D.S.) and the EPSRC and Royal Academy of Engineering for the Award of a Clean Technology Fellowship (K.R.S).

**Supporting Information Available:** Crystallographic data in CIF format. This material is available free of charge via the Internet at http://pubs.acs.org.

IC035350B

(23) Skiba, O. V.; Savochkin, Y. P.; Bychkov, A. V.; Porodnov, P. T.; Babikov, L. G.; Vavilov, S. K. Technology of pyrochemical processing and production of nuclear fuel. *Proceedings of the International Conference on Future Nuclear Systems Global '93*, Seattle, WA, Sept 12−17, 1993; American Nuclear Society: LaGrange Park, Illinois.